THREE-DIMENSIONAL PERMEABILITY DETERMINATION OF REINFORCED COMPOSITES STRUCTURES WITH VERTICALLY ALIGNED CARBON NANOTUBE FORESTS

Ludovic Chevallier*[1], Quentin Govignon[1], Philippe Olivier[2], Gerard Bernhart[1], Jonathan Bouillonnec[1], Martine Mayne-LHermite[3]

[1]*Ecole des Mines Albi-Carmaux, Institut Clement Ader, 81013 Albi CT cedex 09, France*
[2]*Universite de Toulouse, UPS, Institut Clement Ader, 135 avenue de Rangueil F-31077 Toulouse, France*
[3]*CEA, IRAMIS, SPAM, Laboratoire Francis Perrin (CNRS URA 2453), 91191 Gif/Yvette, France*
* *Corresponding Author: ludovic.chevallier@mines-albi.fr*

Keywords: Three-dimensional permeability, aligned carbon nanotubes, algorithm, ethylen glycol

Abstract

By processing aligned carbon nanotube-reinforced composites, ICA intends to exploit their outstanding mechanical properties for ballistic applications. The key challenge is to produce well-sized samples for realistic mechanical tests. This may best be accomplished using a two-stage process that involves first growing vertically-aligned carbon nanotubes (VACNTs) on carbon fibres by catalytic chemical vapor deposition (CCVD) and then infusing multi-scale epoxy composites by vacuum assisted transfert molding (VARTM). It is believed that the inclusion of VACNTs layers of carbon fibre reinforcement could have a severe effect on the preform permeability especialy through the thickness. Despite the relatively small thickness dimension of the composite parts, the use of a distribution layer (DL) in the VARTM process induces very significant though the thickness flow. The purpose of our study is therefore to investigate the effect of VACNTs on three-dimensionnal permeability during molding process and to optimize nano-structured composites production. In preliminary tests epoxy resin is substitued with ethylene glycol as test fluid for reuse and repetability determination, traditionnal preform consisting of three layers of woven carbon fibre fabrics are compared, to nano-structured preform consisting of three layers of the same woven carbon fabrics with VACNTs deposition. The effect of compaction and fibre volume content is taken into account by varying the preform thickness. The permeability is determined using cameras from the top and from the bottom through a full-transparent mould and matching it with simulation using a permeability estimation algorithm (PEA).

1. Introduction

Ballistic applications are an innovative way to promote a new generation of nano-reinforced composites [1][2][3] with the emergence of vertically-aligned carbon nanotubes (VACNTs) [4]. Recent studies show that VACNTs can be oriented according to specific mechanical stress, as it is usually done with carbon fibres. Encouraging progress has been reported compared to

conventionnal materials in the military ballistic protection sector. One of the main remaining issues is to develop a repetable and reliable manufacturing process for those nano-reinforced composites. The choice was made to focus on Liquid Composite Molding process (LCM), this however requires a comprehensive study of permeability properties. A simple measurement system has been designed at ICA for determining three-dimensionnal permeability of large nano-reinforced composites (300x40x0.3 mm), consisting of rigid transparent mould coupled to camera acquisitions from the top and the bottom of the mould, that are then processed by permeability algorithms [5]. To induce through-thickness flow, a distribution layer with a much higher in-plane permeability (K_{xx}) can be placed on top of the preform (Fig. 1). A spacer allows to set the cavity thickness, and control the volumetric fraction of each phase. The Permeability Estimation Algorithm is encoded in Matlab/Simulink Environment and take advantage of the capabilities of PAM-RTM v2013.0 for permeability tensor determination. The permeability is defined according to the Darcy's law:

$$\overline{u} = \frac{-\overline{K}}{\eta}.\nabla P \tag{1}$$

Where u is the Darcy's velocity [m.s^{-1}], K is the permeability tensor [m^2], P is the pressure [Pa], and η is the dynamic viscosity of the resin [Pa.s]. The aim of this study is to characterise the in-plane and through-thickness permeability of woven reinforcement with and without VACNTs deposition.

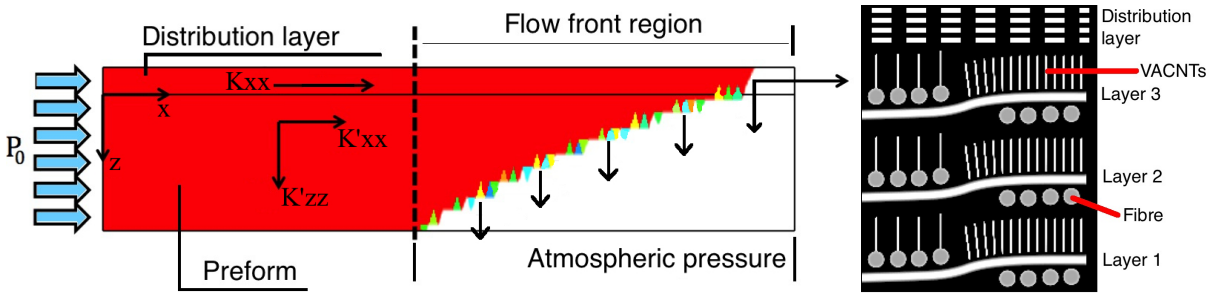

Figure 1. (Left) Sectional view of a simulation of the through-thickness flow in invariant-porosity layers, where K'_{xx} is the in-plane permeability and K'_{zz} is the transverse though-thickness permeability of the preform and P_0 is the injection pressure set at 1,3 atm, $K'_{xx} = K_{xx}.10^{-2}$. (Right) Sectionnal view of the nano-reinforced preform configuration

2. Experimental

2.1. Materials

The nano-structured preforms presented in Fig.2 are obtained by VACNTs forest growth on carbon fabrics via an injection-CVD process at Francis Perrin Laboratory, CEA Saclay, France. The synthesis requires a fibre pretreatment of the carbon fabrics : a SiO_2-based sub-layer deposition at 500°C for a few minutes, and a catalitic decompostion of organic precursors at 850°C, until the expected growth is achieved. While this process will eventually be able to produce larger samples, the materials available for this study were limited to 300x40 mm samples. The thickness of VACNTs forest is in a range of 50-80 μm. The chosen carbon fabric is a 3K 5-harness satin with an areal a weight of 285 g.m^{-2} and a 50/50 warp/weft ratio, purchased from

Test specimens	Nature and treatment
Conventional	5H satin carbon fabric, heat treatment: 500 °C for 5-6 minutes
Nano-reinforced	Carbon nanotubes forest on 5H satin carbon fabric, SiO_2 sub-layer deposition, 500 °C for few minutes + 850 °C for 5 minutes

Table 1. Nature and treatment of the tested specimens

Porcher Industries (ref 3106). To estimate the effect of the VACNTs forest on the woven reinforcement, some fabrics are collected and characterised after a heat treatment at 500°C. Considering the limited availability of nano-structured preforms, a 95:100 ethylen glycol solution is used as a test fluid. This allows tested samples to be recycled, using thermal treatment to evaporate the fluid (120 C for 4-5 hours). Etylen glycol exhibits Newtonian rheological behaviour, and has a viscosity of 16 mPa.s at 25°C (room temperature). The types of tested specimens are describes in Table 1.

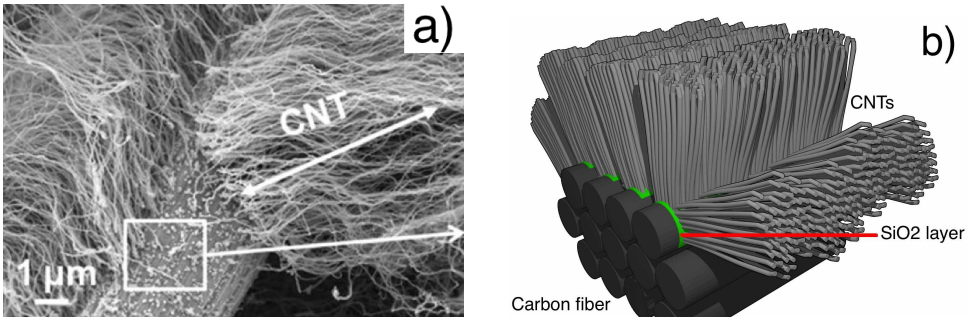

Figure 2. FEG-SEM micrograph of CNTs aligned perpendiculary to the carbon fibre [6] (a) and numerical modelisation of a VACNTs forest rooting in the SiO_2-based sub-layer deposed on carbon fibres (b).

2.2. Procedure

The three-dimensionnal permeability tensor is defined by the following matrix (equ. 2) :

$$K = \begin{bmatrix} K_{xx} & K_{xy} & K_{xz} \\ K_{yx} & K_{yy} & K_{yz} \\ K_{zx} & K_{zy} & K_{zz} \end{bmatrix} \tag{2}$$

The 2D flow configuration permits to evaluate the longitudinal and through thickness permeability. However the use of two materials with different permeabilities prevents direct measurement. Due to the thin and open nature of the DL, K_{zzDL} can be ignored as it is orders of magnitude higher that K_{zzR} K_{xxR}, and is identified in preliminary in-plane measurement tests, by performing a purely 1D infiltration test (Fig. 3). Considering a constant injection pressure, the time-dependant flow front position $x_{(t)}$ in 1D can be defined analytically [7] as the following equation :

$$x_{(t)} = \sqrt{\left(\frac{2KP}{\phi\eta}.t\right)} \tag{3}$$

Where ϕ is the porosity of the different crossed media.The longitudinal DL permeability K_{xxDL} and the trough-thickness reinforcement permeability K_{zzR} are then defined by permeabilty esti-

mation algorithm. The first experiments were performed using ±45°fibres orientation to facili-

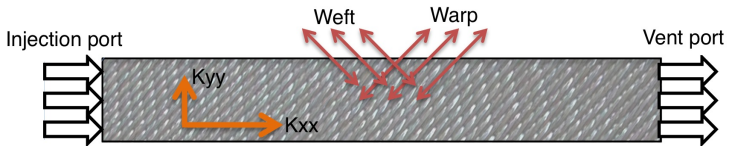

Figure 3. Fibres orientation seen from the top of the preform for in-plane permeability measurement tests.

tate handling and prevent unweaving of the fabric. Samples are constituted of 3 carbon layers, with an added distribution layer on top, with thickness of 0.12 mm. The experiments are repeated for each degree of compaction corresponding to 0.8 mm, 1 mm, and 1.2 mm cavity (Fig. 4). Silicone putties and rubber O-rings are fitted around the sample to prevent race tracking. The ethylen glycol is maintained at constant temperature throughout the measurement process and the temperature is measured for viscosity determination. Injection pressure is measured using two pressure transducers next to the injection and vent port, respectively. The unsaturated flow progression is recorded from the top and the bottom through the PMMA mould Fig.5. After acquisition, the flow data is computed via image analysis to return the flow front coordinates versus time on both side of the mould. The PEA then estimates the permeabilities K_{xxDL} and

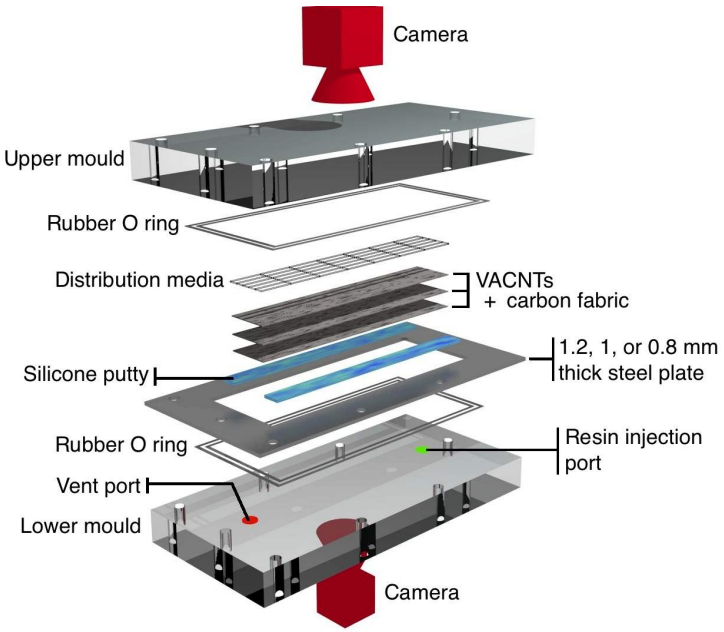

Figure 4. Experimental device associated with permeability estimation algorithm (PEA).

K_{zzR} by iteratively comparing simulation to experimental data: time-dependant progression of the flow front in the distribution layer and distance lag between top and bottom flow front (Fig. 6). The PEA uses Matlab for comparison of experimental and simulated results and integrates PAM-RTM for simulation of the flow. The initial values for simulations are defined by permeability estimation, as explained in table 2: the in-plane permeability K_{xx} of the distribution layer is first defined from experimental data of the time-dependant flow front in the distribution layer (Fig. 6.b.) ploted with equation 3. The permeability can then be determined from the slope of

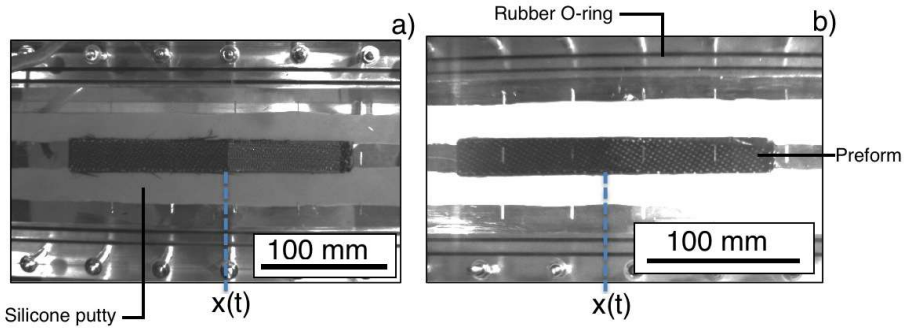

Figure 5. Image acquisition of the flow front in the distribution layer (top) and at the bottom of the preform.

Permeability parameter [m^2]	**Input data**
K_{xxDL} (distribution layer)	Estimation from top flow data
K_{xxR} (preform)	Extrapolation of thickness-dependant permeability
K_{zzR} (preform)	Arbitrary estimation : $(K_{xxR})/10$

Table 2. Determination method of initial permeability values for simulating.

the regression line of $x_t = f_{(t)}$ with the equation 4.

$$K = \frac{\phi\eta}{2P} x_{(t)}^2 \tag{4}$$

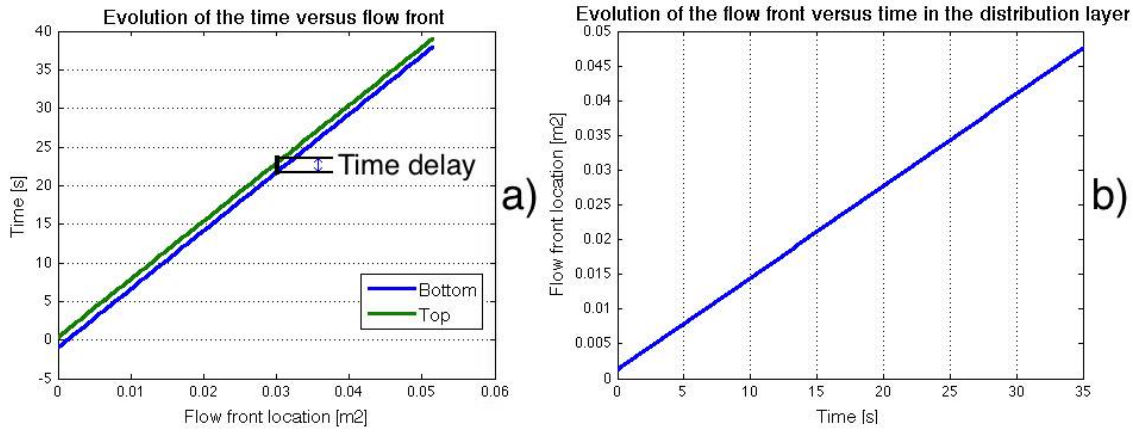

Figure 6. Experimental input parameters to PEA: (a) distance lag between the top front and the bottom front and (b) time dependant flow front in the distribution layer.

As the presence of DL changes the compaction of the fibrous reinforcement, the in-plane permeability of the preform is determined from extrapolation of the volume fraction dependant permeability Fig. 7.

After primary simulation with input parameters Table 3, a relative error E and his absolute value E_{abs} are calculated between experimental and numerical outputs (time delay and flow front in

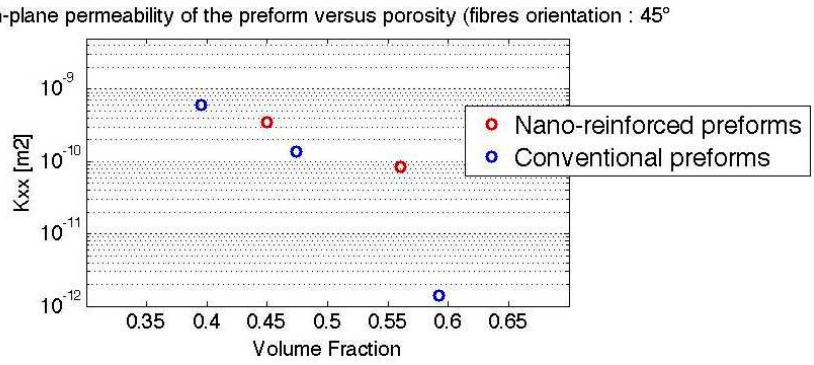

Figure 7. First in-plane permeability measurements versus the volume fraction of carbon fabric in the preform (fibres orientation: ±45 °)

Parameter	conventionnal	nano-reinforced
Distribution layer porosity (PET) []	0.69	0.69
Distribution layer in-plane permeability [m^2]	8.14E^{-10}	8.14E^{-10}
Distribution layer thickness [m^2]	1.2E^{-4}	1.2E^{-4}
Preform Volume fraction []	0.48	0.65
Preform in-plane permeability K_{xx} [m^2]	1.75E^{-10}	6.55E^{-12}
Preform transverse permeability K_{zz} [m^2]	1E^{-12}	1E^{-12}
Overall dimensions (length/thickness) [m]	15.E^{-3}/1.E^{-3}	15.E^{-3}/1.E^{-3}
Number of nodes	25 000	25 000

Table 3. Input parameters for primary simulation

DL), the permeability values are then updated at each iteration and a new simulation is started. The iteration loop stops when the relative error is lower than a convergence criterion ε. The Fig.9 presents the relative error versus iteration number when starting with purely arbitrary input permeability values, the convergence criterion is reached in a dozen iterations. The average time of each PAM-RTM simulation is around 30 seconds on a HP Z600 Quad Core Workstation (2,40 GHz, 8 GB DDR3) with a 25 000 nodes mesh and one used processor. The average convergence time of the PEA is around 7 minutes.

3. Results and discussion

The 1D experiments of in-plane permeability measurements were conducted with 3-layers conventionnal preforms, with volume fraction of 0.592, 0.474 and 0.395 for 0.8 mm, 1 mm, and 1.2 mm spacer respectively. The corresponding in-plane permeabilities were determined at 1.4E^{-12}, 1.36E^{-10} and 6.02E^{-10}m^2 (Fig 7). Due to the VACNTs inclusion, the nano-reinforced preforms presented quite different volume fraction : 0.558 and 0,451 for 1 mm and 1.2 mm spacer respectively. The in-plane permeability were determined at 8.33E^{-11} and 3.5E^{-10} with a volume fraction of 0.558 and 0.451. By exponential regression, the two specimens exhibits close variation. This observation could be attributed to the small size of the VACNTs that prevent an important variation of the flow front propagation. The first transverse permeability tests resulted in measurement of 1.64E^{-13} m^2 and 1.07E^{-12} m^2 for the conventionnal and the nano-reinforced preform, with a volume fraction of 0.48 and 0.65, respectively. The through-thickness per-

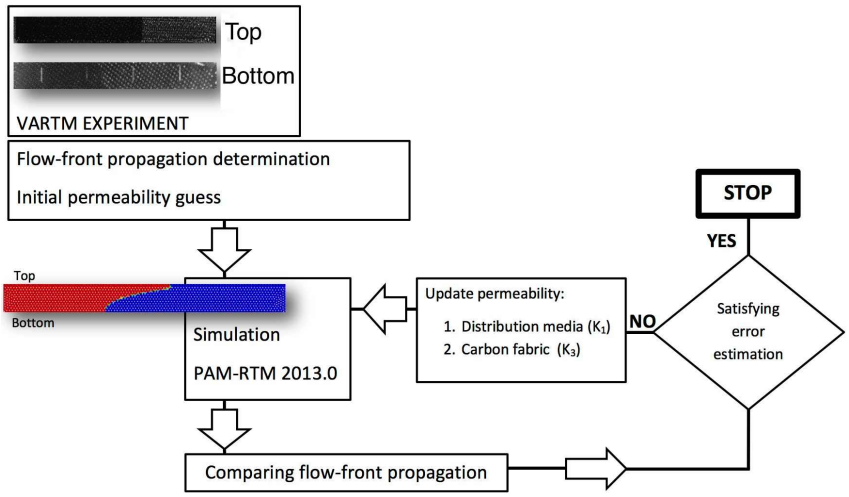

Figure 8. Flowchart of the Permeability Estimation Algorithm.

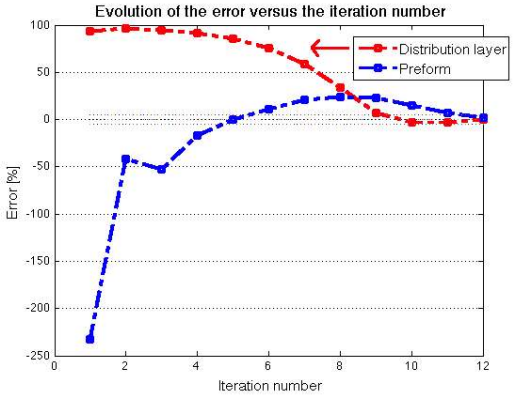

Figure 9. K_{xxDL} and K_{zzR} convergence (ε=0.03)

meability unexpectedly appears lower for the VANCTs fabrics whilst it has a higher volume fraction, this can be the result of the VACNTs orientation allowing an easier transverse flow from one layer to the next. Further experiments are needed to define a global variation of K_{zzR} depending on the volume fraction and also assess the effect of preform orientation. The difference of heat treat treatment could result in a difference of the wettability between conventionnal and nano-structured performs. The surface density of the VACNTs has a strong influence to the forest porosity and the flow front propagation through the thickness which will need to be evaluate.

4. Conclusion

The use of ethylen glycol, conditioned by the limited availability of nano-reinforced samples, permited to execute the first permeability measurement with a fibre orientation at ±45°, and to observe the variation of the in-plane and through-thickness permeability by VACNTs inclusion. In this context, a robust permeability estimation algorithm has been presented, easily applicable to other nature of materials. The coupling between in-plane and transverse permeability measurement is an efficient way to characterise the RTM manufacturing properties of the woven

Permeability parameters [m^2]	Conventionnal	Nano-reinforced
K_{xx} (DL)	7.65E^{-10}	4.96E^{-10}
K_{xx} (preform)	1.75E^{-10}	6.55E^{-12}
K_{zz} (preform)	1.64E^{-13}	1.07E^{-12}

Table 4. Output permeability values determined by PEA (1mm air cavity, fibres orientation ±45)

fabrics. The actual experimental results have showed a small variation of in-plane permeability between conventionnal and nano-reinforced carbon fabrics. The transverse permeability will require further experiments to determine the influence of inter-layer VACNTs forest. The RTM manufacturing process can easily be applied to the nano-reinforced composites domain, however requiring specific safety rules.

5. Aknowledgements

The authors are thankful to Martine Mayne-LHermite of Francis Perrin laboratory, CEA Saclay and her staff, for providing nano-reinforced materials for this study, and to DGA for reasearch grant for the IN'PACT project.

References

[1] S. RAHMANIAN, A.R. SURAYA, R. ZAHARI, and E.S. ZAINUDIN. Synthesis of vertically aligned carbon nanotubes on carbon fiber. *Applied Surface Science*, 271(0):424 – 428, 2013.

[2] M. GRUJICIC, W. BELL, L. THOMPSON, K. KOUDELA, and B. CHEESEMAN. Ballistic-protection performance of carbon-nanotube-doped poly-vinyl-ester-epoxy matrix composite armor reinforced with e-glass fiber mats. *Materials Science and Engineering: A*, 479(12):10 – 22, 2008.

[3] S. LAURENZI, R. PASTORE, G. GIANNINI, and M. MARCHETTI. Experimental study of impact resistance in multi-walled carbon nanotube reinforced epoxy. *Composite Structures*, 99(0):62 – 68, 2013.

[4] M. KUMAR and Y. ANDO. Chemical vapor deposition of carbon nanotubes: A review on growth mechanism and mass production. *Journal of Nanoscience and Nanotechnology*, 10(6):3739–3758, 2010.

[5] Ali GOKCE, Mourad CHOHRA, Suresh G. ADVANI, and Shawn M. WALSH. Permeability estimation algorithm to simultaneously characterize the distribution media and the fabric preform in vacuum assisted resin transfer molding process. *Composites Science and Technology*, 65(14):2129 – 2139, 2005.

[6] M. DELMAS. Growth of long and aligned multi-walled carbon nanotubes on carbon and metal substrates. *Nanotechnology*, 23, 2012.

[7] Jamal ECHAABI Mohamed HATTABI and Mohamed OUADI BENSALAB. Experimental analysis of the resin transfer molding process. *Korea-Australia Rheology Journal*, 20(1):7 – 14, 2008.